Pharmaceutical Research, Volume 23, No. 2, February 2006 (© 2006)
DOI: 10.1007/s11095-005-9225-1

Research Paper

Specific Delivery of Corroles to Cells via Noncovalent Conjugates with Viral Proteins

Hasmik Agadjanian,[1] Jeremy J. Weaver,[2] Atif Mahammed,[3] Altan Rentsendorj,[1] Sam Bass,[1] Jihee Kim,[4] Ivan J. Dmochowski,[5] Ruth Margalit,[5] Harry B. Gray,[2] Zeev Gross,[3] and Lali K. Medina-Kauwe[1,6]

Received July 14, 2005; accepted October 21, 2005

Purpose. Corroles are amphiphilic macrocycles that can bind and transport metal ions, and thus may be toxic to cells. We predicted that anionic corroles would poorly enter cells due to the negatively charged cell membrane, but could be ideal tumor-targeted drugs if appropriate carriers enabled delivery into tumor cells. In this work, we test the hypothesis that recombinant cell penetrating proteins of the adenovirus (Ad) capsid form noncovalent conjugates with corroles to facilitate target-specific delivery and cell death.
Methods. Corroles mixed with recombinant proteins were tested for conjugate assembly, cell penetration, stability, targeted binding, and cell killing *in vitro*.
Results. Sulfonated corroles entered cells only with carrier proteins, and formed stable complexes with recombinant Ad capsid proteins. ErbB receptor-targeted conjugates were cytotoxic to ErbB2-positive but not ErbB2-negative breast cancer cells, whereas molar equivalents of free corrole had no effect on these cells.
Conclusions. Sulfonated corroles are cytotoxic to ErbB2-positive breast cancer cells when delivered by a targeted cell penetrating protein. The relatively low dose required to accomplish this compared to untargeted compounds suggests that corroles may lend themselves to targeted therapy. Importantly, the amphiphilicity of corroles enables a unique approach to bioconjugate formation whereby the carrier and drug form a stable complex by noncovalent assembly.

KEY WORDS: capsid; corrole; metal; penton base; targeting.

INTRODUCTION

We report the use of corroles as novel drugs that can readily bind shuttle proteins noncovalently and induce targeted toxicity to certain cells in culture. Corroles are macrocyclic compounds with structural similarity to porphyrins, and, likewise, can chelate a large variety of metal ions. Whereas porphyrins have been used extensively in cancer therapy (1–3), corroles have not been explored until recently, when the once-complicated methodology for their synthesis became simplified (4,5). The production of amphiphilic, water-soluble corroles now enables investigations of these compounds for application in physiological environments. The unique features of corroles that should lend themselves to bioconjugate therapy are: tight noncovalent binding to proteins in solution, highly intense fluorescence, and poor cell uptake without a carrier molecule.

A hallmark feature shared by several recently introduced corroles is amphiphilicity, enabled by negatively charged moieties positioned on one side of the macrocycle. These negative charges are likely to prevent nonspecific uptake of corroles into cells without the aid of a carrier. Many serum molecules could be potential carriers of corroles systemically, as porphyrins and related compounds are known to transport into cells by serum proteins (6,7). It has been shown that the sulfonated corroles explored in this study bind rapidly and noncovalently to human serum albumin (HSA), forming extremely stable complexes that remain associated during high-performance liquid chromatography (HPLC) separation (8).

To take advantage of the capacity for such stable interactions with proteins, we asked in this study whether corroles could form noncovalent conjugates with specific receptor-targeted proteins known to penetrate into cells. We also asked whether ligand-directed delivery of corroles could induce targeted cell death. Here we show that corroles readily interact with the recombinant proteins tested in this study,

[1] The Gene Therapeutics Research Institute, Cedars-Sinai Medical Center, 8700 Beverly Blvd, Davis 5092, Los Angeles, California 90048, USA.
[2] Department of Chemistry, California Institute of Technology, Pasadena, California 91125, USA.
[3] Department of Chemistry, Technion – Israel Institute of Technology, Haifa 32000, Israel.
[4] IntraGene Sciences, Institute for Genetic Medicine, Los Angeles, California 90033, USA.
[5] Department of Chemistry, University of Pennsylvania, Philadelphia, Pennsylvania 19104, USA.
[6] To whom correspondence should be addressed. (e-mail: MedinaL@cshs.org)

but do not transfer to serum albumin after conjugate assembly. Importantly, we show that these recombinant proteins direct the receptor-targeted cell binding and cell entry of corroles, eliciting specific cell death after corrole delivery.

Among the recombinant carrier proteins tested here are derivatives of the Adenovirus serotype 5 (Ad5) capsid penton base protein: PB, PBK10, and HerPBK10. PB is a recombinant protein encompassing the entire amino acid sequence of the wild-type Ad5 penton base (9,10), and is known to mediate cell entry of the virus during infection. PBK10 carries the wild-type penton base sequence followed by a carboxy (C)-terminal decalysine (9). Both PB and PBK10 interact with cellular integrins and undergo integrin receptor-mediated cell entry (9). A heregulin-targeted version, HerPBK10, specifically binds heregulin, or ErbB, receptors that are amplified on the cell surface of ErbB2+ human breast cancer cells, including MDA-MB-435 and MDA-MB-453 cell lines, and undergoes receptor-mediated cell entry (11–13). Importantly, these proteins were derived from the penton base because of its capacity for endosomolysis and translocation into the cytosol, which should facilitate targeted entry of the corrole into the cell interior. Also relevant to this study is the protein, Her, which encompasses the receptor binding domain of heregulin-α and competitively inhibits HerPBK10 binding to heregulin receptors (11).

We have previously demonstrated that HerPBK10 delivers plasmid DNA molecules to ErbB2+ cells through a mechanism involving ErbB receptor-specific binding and endocytosis, and endosomal escape, likely via the PB domain of HerPBK10 (11). Delivery of plasmid DNA, however, presents certain barriers to potential therapy. For example, the large size of the DNA molecule requires that DNA condensing agents be added to assembled complexes to collapse the plasmid into a particle (14,15). Such agents are likely to bind DNA very tightly and may, ironically, hamper gene expression as a result of this interaction (16). Moreover, even if such agents are able to release DNA inside the cell cytoplasm, the uncondensed molecule is unable to migrate through the crowded cytosol toward the nucleus (17). The attachment of a cytotoxic molecule to HerPBK10, on the other hand, may streamline conjugate design and assembly. Attachment via noncovalent interactions, as tested here, would greatly simplify delivery of therapeutic molecules.

This study presents three areas of novelty: (1) the testing of corroles on a biological system; (2) the noncovalent assembly of corroles with recombinant cell targeting proteins; (3) the demonstration that corroles can be targeted to specific cell surface receptors, eliciting cell death. Here we present our *in vitro* findings.

MATERIALS AND METHODS

Materials

Phosphate buffered saline (PBS), PBS: 137 mM NaCl, 2.7 mM KCl, 4.3 mM Na_2PO_4, 1.4 mM KH_2PO_4. PBS, Mg^{2+}/Ca^{2+}: PBS supplemented with 0.01% final $CaCl_2$ and $MgCl_2$. The corrole compounds S2FB, S2Ga, and S2Mn were synthesized as described elsewhere (4,5). Corroles were reconstituted in PBS and concentrations quantified by obtaining the λ_{max} absorption using UV–Vis spectroscopy and applying the equation: (absorbance at λ_{max} / corrole extinction coefficient) × dilution factor = concentration (M). The extinction coefficients at λ_{max} of each corrole are listed in Table I. HeLa, 293, MDA-MB-453 (ErbB2+), MDA-MB-435 (ErbB2+), and MDA-MB-231 (ErbB2−) cells were maintained in complete media, consisting of DMEM supplemented with 10% fetal bovine serum and penicillin/streptomycin at 37°C, 5% CO_2. PB, PBK10, HerPBK10, and Her recombinant proteins were produced as histidine-tagged fusion proteins, as described previously (9,11,13). After metal chelate affinity chromatography of HerPBK10, the protein eluate was further purified from smaller molecular weight products by HPLC using a size exclusion column (TSKgel G 3000 SWXL, 7.8 mm × 30 cm; Tosoh Bioscience, Montgomeryville, PA, USA). Elution of proteins was monitored at 280 nm at a flow rate of 1 mL min^{-1}, and the fraction eluting at 6 min (delineating full-length HerPBK10) was used for subsequent conjugate assembly. Protein concentrations quantified using a Micro-BCA protein assay kit (Pierce Biotechnology, Inc., Rockford, IL, USA) and measuring absorbance at 560 nm.

Corrole Uptake Assay

HeLa, or 293 (1×10^4/well), or MDA-MB-453 (5×10^4/well) were plated in 96-well dishes and grown overnight. The next morning, the media was replaced with 0.1 mL final volume of 27 μM S2FB in PBS, Mg^{2+}/Ca^{2+} with or without 5 μM PB, or Lipofectin (2 μg) per well. The cells were incubated for 30 min to 1 h at 37°C, then observed immediately by fluorescence microscopy without prior washing. In previous experiments, we tried washing the cells to remove the background fluorescence, but most of the cells were loosely attached to the substratum because of the PB binding to integrins in protein-free buffer. It is well established that the penton base can bind integrins and thus cause cell lifting, whereas the cells otherwise remain viable (18,19). Our experience with this protein suggests that this effect is less

Table I. Summary of Corroles

Name of corrole	Fluorescent	Metallated	Type of metal	λ_{max} Absorbance	Extinction coefficient (cm^{-1} M^{-1})
S2FB	Yes	No	–	430	60,000
S2Ga	Yes	Yes	Gallium	424	74,700
S2Mn	No	Yes	Manganese	420	21,000

pronounced in complete (i.e., serum-containing) cell media than in protein-free buffer.

For uptake in complete (serum-containing) media, S2Ga was added at 3 μM final concentration directly to the cell medium, then cells were incubated at 37°C in the dark at 5% CO_2 for at least 30 min, after which the cells were directly visualized under the microscope. To measure cytotoxicity after treatment in complete media, each cell line was plated in seven 96-well plates (to measure one plate/day) at 1×10^4 cells well^{-1} in 0.2 mL well^{-1}, and allowed to grow for 24 h before treatment. On day 0, the media was aspirated and fresh media added containing the indicated concentration of corrole in 0.2 mL well^{-1}, in triplicate wells. Importantly, all cells were incubated in the dark and did not receive prolonged exposure to light. On each subsequent day (i.e., day 1, day 2, etc.), an ELISA-based BrdU incorporation assay was performed on sequential plates following the manufacturer's instructions (Exalpha Biological, Inc., Watertown, MA, USA). The reactions were measured at 460 nm using a SpectraMax M2 plate reader (Molecular Devices Corp., Sunnyvale, CA, USA).

Conjugate Assembly

Proteins were conjugated with sulfonated Ga, Mn, and freebase corroles by separately incubating indicated proteins with 10 times molar excess of corroles at room temperature for 1 h on a slow shaker, protected from light. The unbound corroles were removed by ultrafiltration through 10 K MW cutoff spin column filters (Millipore Corporation, Billerica, MA, USA) according to the manufacturer's procedures for diafiltration, and the conjugates washed with PBS until the filtrate clarified. The retentates retained their bright green color (indicative of corrole pigment) throughout the filtration process. The retentates were resuspended in PBS and measured for absorbance at the λ_{max} of the corrole to obtain the corrole concentration as described earlier. Whereas the λ_{max} of S2Ga, for example, shifts from 424 to 429 nm when bound to proteins, this does not dramatically change the estimation of corrole concentration in complexes.

Testing for Equilibration with Bovine Serum Albumin

The wells of a 96-well dish were prepared using established methodology for standard immunoassays. Briefly, wells were coated with bovine serum albumin (BSA) at 2 μg well^{-1} and allowed to adsorb overnight. The next morning, the wells were emptied and rinsed with PBS. PBK10-S2Ga conjugates were prepared by incubating 20 μg PBK10 with 60 nmoles S2Ga and ultrafiltering as described earlier. PBK10-S2Ga was added to triplicate wells of the BSA-coated dish at an equivalent final concentration of 2 μg of PBK10 per well. A separate triplicate set of wells received S2Ga alone at 15 nmoles of S2Ga per well. The dishes were incubated at room temperature for 30 min with agitation. The samples were then removed from the wells and their absorbances at 424 nm were measured to determine the remaining corrole concentration in each sample after incubation with BSA-coated wells. The absorbance at 424 nm of the wells was also measured after sample removal to determine if there was any residual corrole left in the wells after sample removal.

To test for transfer of corroles to BSA from immobilized conjugates, PBK10-S2Ga conjugates were prepared as described earlier, then bound to PBS-equilibrated Ni-NTA agarose beads (Qiagen, Inc., Valencia, CA, USA) in 0.2 mL volumes (in triplicate) by incubation in tubes on ice with agitation for 1 h. The tubes were centrifuged at $1{,}000 \times g$ for 2 min, washed with PBS to removed unbound conjugate, then incubated with either 0.5 mg mL^{-1} BSA in PBS or PBS alone for 30 min at room temperature with gentle agitation. The tubes were centrifuged and supernatants ("filtrates") collected. The beads were then incubated with elution buffer (9,11,13) to elute the conjugates from the beads, and the eluates were collected. The absorbance of filtrates and eluates were measured at 424 nm on a plate reader (SpectraMax M2; Molecular Devices).

Cell Targeting Assays

To assay the cellular uptake of complexes, we plated 5×10^4 MDA-MB-453 per well (in 100 μL well^{-1}) in 96-well dishes and grew the cells overnight. We added 20 μL (36 pmol HerPBK10-S2Ga complex) to wells on ice (to promote receptor binding but prevent receptor internalization). The cells were then warmed to 37°C up to 45 min (to promote endocytosis of receptors and their bound ligands). The cells were given a mild acid wash at the following time points of warming: 0, 5, 15, 30, and 45 min at 37°C to remove any nonspecifically bound protein. Specifically, wells received 100 μL of 0.25 M acetic acid, 0.5 M NaCl, then after 10 s, neutralized with 50 μL of 1 M Na acetate. After washing with PBS, Mg^{2+}/Ca^{2+}, the cells were observed under fluorescence microscopy. To obtain cells with complexes that are bound on the cell surface only, and not internalized, a set of cells were incubated on ice with the complexes, then washed with PBS, Mg^{2+}/Ca^{2+} without receiving a mild acid wash.

To test the competitive inhibition of receptor binding and uptake, we plated 5×10^4 MDA-MB-453 in 96-well dishes and incubated the cells overnight. The dishes were then placed on ice and we coincubated 36, 360, or 1,800 pmol Her on cells with 36 pmol of either HerPBK10-S2Ga or BSA-S2Ga. After 30 min on ice, the cells were washed with PBS, Mg^{2+}/Ca^{2+} to remove nonspecifically bound proteins, then warmed to 37°C for 5 min to promote internalization. Afterwards, complexes remaining on the cell surface were removed by a mild acid wash, as described earlier. A solution of 5× diluted trypan blue was added to the cells in PBS at room temperature for 5 min, then the cells were washed in PBS, Mg^{2+}, visualized live under brightfield and fluorescence microscopy, and then quantified by scoring. We scored ≥100 cells per field in three independent fields per treatment, and determined the percentage of red fluorescent cells out of the total cells scored from each field.

To test targeted toxicity, MDA-MB-435 and MDA-MB-231 cells were first plated in 96-well plates at 1×10^4 cells well^{-1}. At 48 h after plating, sets of wells were aspirated and received 0.1 mL of the following: media only (untreated control) or 0.5 μM (with respect to corrole concentration) of HerPBK10-S2Ga or HerPBK10-S2Mn. For the wells receiving the Her competitive inhibitor, the cells were preincu-

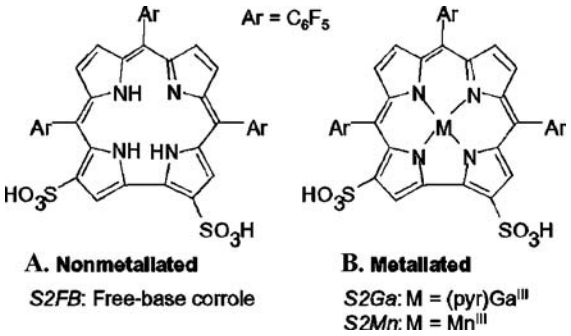

Fig. 1. Chemical structure of the (A) nonmetallated free base and (B) metallated corroles tested in this study.

bated with Her at a 10-fold molar excess (in comparison to HerPBK10 in the conjugates) for 1 h on ice to promote receptor binding, after which the conjugates were added and incubated on the cells for 4 h at 37°C. Afterwards, free conjugates were aspirated and 0.2 mL of fresh media added. For comparison against nontargeted corroles, cells received equivalent concentrations (0.5 μM) of S2Ga alone or as a BSA-S2Ga conjugate. All wells received this treatment daily, whereas each day a separate set of wells were measured for cell survival using a kit for measuring metabolic activity (BioAssay Systems, Hayward, CA, USA).

Microscopy

Fluorescent cells were visualized using an Olympus IMT-2 inverted microscope fitted with a Texas Red filter. Confocal imaging of cells containing corroles were obtained using an inverted laser scanning confocal microscope (Leica Microsystems Heidelberg, Mannheim, Germany). Samples were excited by UV and captured in a 600–656 emission window.

To visualize intracellular corrole by confocal microscopy, HeLa cells were plated on coverslips at 1×10^5 cells per well in 6-well dishes. At 48 h after plating, S2Ga was added directly to the cell media at 15 μM final concentration, and incubated for 45 min at 37°C, 5% CO_2, in the dark. The cells were then aspirated of media, washed with PBS, Mg^{2+}, then coverslips were directly placed on slides and viewed by confocal microscopy. HeLa cells were chosen for this microscopy because of their flat nature and large cytoplasm. We have attempted to visualize MDA-MB-453 cells by confocal microscopy; however, these cells are not morphologically conducive to this methodology because they are too round, making the cytoplasm difficult to visually isolate.

RESULTS

Carrier Molecules Appear to Facilitate Corrole Uptake

The corroles under investigation carry two sulfonates, and have been synthesized as a nonmetallated freebase compound, designated S2FB (Fig. 1A), and as metallated compounds, designated S2Ga and S2Mn (Fig. 1B). S2FB is a brightly fluorescent freebase molecule (20). S2Ga is bound to a gallium metal group and is even more fluorescent (20). S2Mn carries manganese and is nonfluorescent (Table I).

To test whether corroles readily penetrate the cell membrane, we took advantage of the fluorescence of the S2FB molecule to track uptake. Several cell lines (HeLa, 293, and MDA-MB-453 cells) were incubated in protein-free buffer containing S2FB (27 μM) alone (Fig. 2A–C), or with the cell entry protein, PB (at 5 μM) (Fig. 2D–F). In the absence of PB, the concentration of corrole in the media

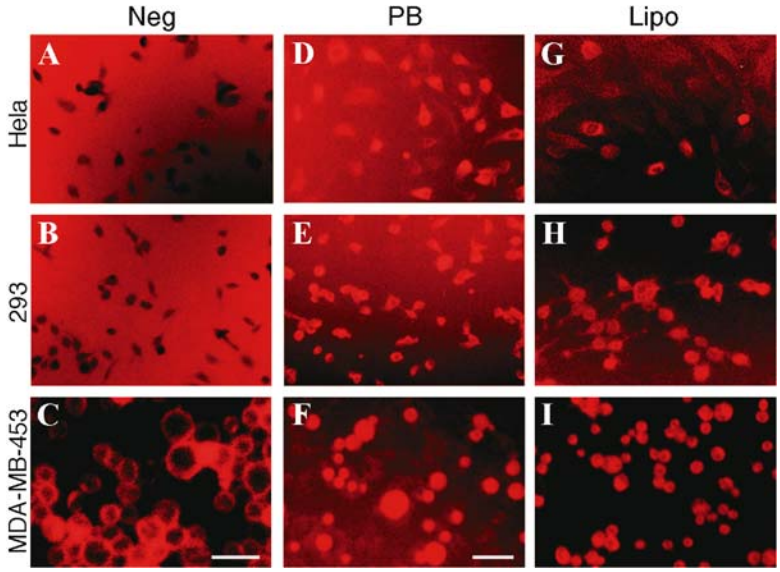

Fig. 2. Corrole uptake requires a carrier. (A–I) Cells were treated by corroles in buffer only (Neg) or with recombinant penton base (PB) or Lipofectin (Lipo). Images were obtained of live cells at 10× magnification using a fluorescence inverted microscope. Fluorescence settings were kept constant between imaging, and images were captured at constant exposure and gain settings. C and F are slightly enlarged views. Bar, ~20 μm.

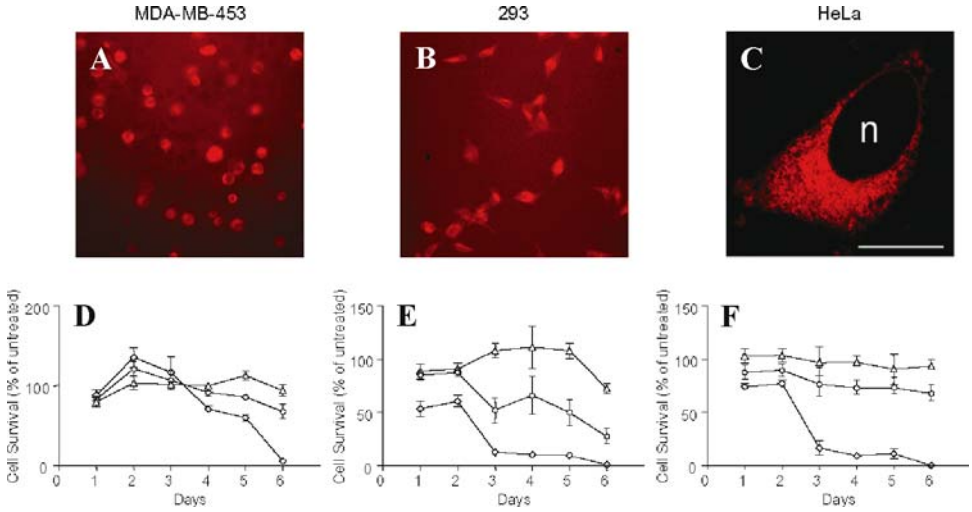

Fig. 3. S2Ga uptake and cell death. (A, B) Fluorescence microscopy of live cells 30 min after addition of 3 μM final S2Ga directly to cell media, as described in Materials and Methods. (C) Live cell confocal fluorescence microscopy of HeLa cell after S2Ga (15 μM final) uptake in complete media, as described in Materials and Methods. (D–F) Analysis of cell survival by cell proliferation assay on (D) MDA-MB-435, (E) 293, and (F) HeLa cells. Cells were treated daily with 0.3 μM (triangles), 3 μM (circles), and 30 μM (diamonds) S2Ga added directly to cell media, as described in Materials and Methods.

seemed much greater than in the cells. In contrast, coincubation with PB yielded an enhanced cellular corrole fluorescence. Although S2FB seemed to adhere to the surface of MDA-MB-453 cells in the absence of PB, coincubation with PB, once again, seemed to enhance cellular corrole fluorescence. The transfection agent, Lipofectin (at 2 μg), which is normally used to facilitate cell entry of exogenous nucleic acids, produced similar results (Fig. 2G–I).

Complete (i.e., serum-containing) cell medium alone also seemed to facilitate the uptake of S2FB (not shown), and S2Ga into MDA-MB-453, 293, and HeLa cells (Fig. 3A–C). To confirm whether we were observing intracellular, as opposed to cell-bound, S2Ga fluorescence, we examined HeLa cells live using laser scanning confocal fluorescence microscopy after uptake in complete medium. The flat morphology and large cytoplasm of HeLa cells, and the brighter fluorescence intensity of S2Ga together facilitated confocal imaging. Imaging a section of the cell through both the cytoplasm and nucleus, we observed that the corrole accumulated in the cytoplasm, but remained excluded from the nucleus (Fig. 3C).

After several days in complete medium, high (30 μM) concentrations of S2Ga reduced 293, HeLa, and MDA-MB-435 cell numbers by 95–100%, whereas low concentrations (3–0.3 μM) had modest to no effect (Fig. 3D–F). Identical concentrations of S2FB had no effect on MDA-MB-435 cells, whereas S2Mn had no effect on 293 and HeLa cells (not shown).

These initial findings suggested that corroles could induce cell death after cell entry, and could enter the cell either by fluid co-uptake with a carrier, or as a bound conjugate to a carrier. As corroles are capable of noncovalent interactions with proteins, we investigated whether corroles could form conjugates with targeted cell entry proteins (Table II).

Corroles Form Stable Conjugates With Recombinant Cell Entry Proteins

To determine whether noncovalent conjugates form between S2Ga and recombinant proteins, we incubated the following proteins with S2Ga: (1) PB, (2) PBK10, (3) HerPBK10, (4) Her, and (5) BSA. We mixed 20 μg of each protein with the indicated concentrations of S2Ga and incubated the mixes for 30 min at room temperature to allow the corrole to bind with each protein. Free, unbound corrole

Table II. Summary of Carrier Molecules

Name of reagent	Description	Purpose
BSA	Bovine serum albumin	Nonspecific carrier
Lipofectin	Transfection reagent	Nonspecific permeabilization of cells
PB	Ad5 capsid penton	Integrin binding, cell entry, and endosomolysis
PBK10[a]	Polylysine-tagged penton	Integrin binding, cell entry, and endosomolysis
Her[b]	Heregulin receptor ligand	Heregulin receptor binding and cell entry
HerPBK10[c]	Heregulin-targeted penton	Heregulin receptor binding, cell entry, and endosomolysis

[a] Medina-Kauwe *et al.* (9).
[b] Medina-Kauwe *et al.* (13).
[c] Medina-Kauwe and Chen (12).

Table III. Assembly of Protein–Corrole Complexes

Protein (name)	Protein (μg)	S2Ga input (nmol)	S2Ga retentate (nmol)	S2Ga/Protein (mol:mol)
BSA	20	7	5.6	18.7
Her	20	7	5, 3.2	5.6, 3.6
HerPBK10	20	7	4.9, 1.9	24.5, 9.5
PB	20	7	8, 3	26.7, 10
PBK10	20	7	4.1, 9.4	13.7, 31.3

The indicated concentrations of reagents were mixed together in a 0.5-mL final volume of PBS and processed according to the protocol described in Materials and Methods for conjugate assembly. Except for the BSA conjugate, each experiment was performed twice, independently. Thus, the results for the S2Ga retentates and corrole/protein ratios are given as two numbers, one from each independent experiment. Except for BSA, each complex was assembled twice and measured by UV–Vis absorbance. Although in two cases, it appears that the retentates contain more corrole than the original input amount, these findings suggest that the actual input concentration of corrole may be slightly higher than the theoretical input amount.

was removed by ultrafiltration through a size exclusion membrane. As determined by measuring the absorbances of retentates at specified wavelengths, it was evident that each protein molecule could bind and retain multiple corrole molecules throughout the filtration process (Table III). Importantly, these findings suggest that the binding of S2Ga to proteins is strong enough to withstand ultrafiltration and buffer exchange.

As a further verification of conjugate formation, we mixed HerPBK10 and S2FB, filtered the mixture as described above, then ran the retentate through a size exclusion column by HPLC, monitoring elution at 280 and 422 nm to identify protein and corrole maximum absorbances, respectively. HerPBK10 and S2FB alone were also each applied separately to the column. S2FB alone elutes at ~12 min, but when combined with HerPBK10, the elution time of S2FB is shifted to ~6 min (Fig. 4B), which is the same elution time as that of HerPBK10 alone (Fig. 4A). Importantly, although the full-length HerPBK10 protein elutes at 6 min whereas smaller-sized products elute at later time points, the fraction collected only at 6 min was used for subsequent conjugate assembly.

The retention of corrole binding to protein during ultrafiltration and HPLC purification suggests that the interaction is highly stable. As an additional examination of stability, we determined whether corroles transfer from the conjugate to serum proteins. For this assay, we first formed complexes between PBK10 and S2Ga as just described earlier. The complexes were then applied to BSA-coated wells at 2 μg of PBK10 per well, with each well containing 2 μg of immobilized BSA. PBK10 and BSA have similar molecular weights, and were thus used in equivalent molar concentrations in this assay. Noncoated wells were included as controls for nonspecific binding of corroles or conjugates to the well surface. After incubation in the wells for 30 min, we removed the complexes and measured their absorbance at 424 nm. We also measured the absorbance of the wells containing the immobilized BSA after complex removal. We reasoned that if the corrole was released from PBK10 and bound to the BSA, we would lose significant corrole absorbance to the immobilized BSA and see a marked reduction in complex absorbance in comparison to complexes not exposed to the BSA. Our findings show a 9.4% gain of absorbance by the BSA and nearly 90% retention of absorbance by PBK10, indicating little exchange of corrole between the proteins (Fig. 5A). This is in agreement with previous studies showing nanomolar dissociation constants for corrole–protein complexes (8). If the conjugate nonspecifically bound to the well surface, and the BSA blocked these adsorption sites, there would be significant increase in corrole absorbance by the noncoated (−BSA) well compared to the coated (+BSA) well, and likewise significant loss of absorbance from the conjugate sample after removal from the −BSA compared to the +BSA well. However, this did not seem to be the case.

As a confirmation of stability, we immobilized PBK10-S2Ga complexes on nickel beads via the polyhistidine affinity tag engineered into the PBK10 protein. The beads were washed with either PBS alone or PBS containing 0.5 mg mL^{-1} BSA, and the filtrate absorbances were measured at 424 nm. The complexes were then eluted from the nickel beads and eluate absorbances also measured. Consistent with the previous findings, there was little to no gain of absorbance by the BSA wash compared to PBS alone. Likewise, the BSA solution produced little to no loss of absorbance from the conjugates compared to PBS alone (Fig. 5B).

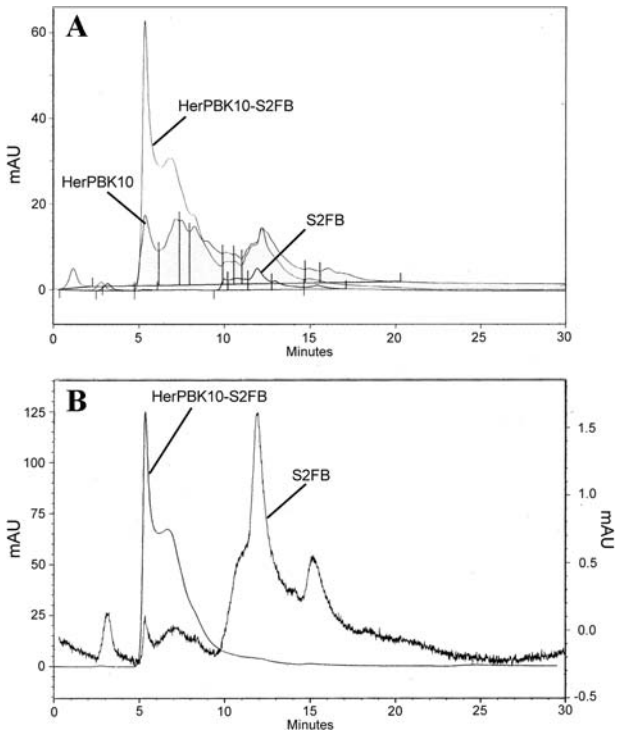

Fig. 4. Assembly of corrole conjugates. Conjugate assembly was assessed by HPLC of conjugates (HerPBK10-S2Ga) or separate conjugate components (HerPBK10, S2Ga) through a size exclusion column. Elution of compounds was monitored at (A) 280 nm and (B) 422 nm to measure protein and corrole, respectively. In panel (B), the absorbance of the conjugate or corrole alone is measured against the left or right *y*-axis, respectively.

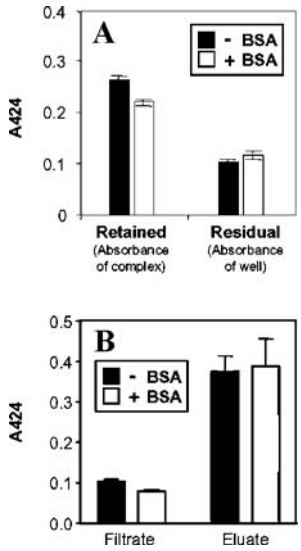

Fig. 5. Corrole binds tightly to carrier, with negligible transfer to BSA. Corrole loss from PBK10-S2Ga conjugate is reflected by the difference between the filled and open bar of the "Retained" category. Likewise, corrole gain by BSA is reflected by the difference between the filled and open bar of the "Residual" category. The presence of S2Ga was detected by measuring absorbance at 424 nm.

In the remaining studies, the name of each conjugate is designated by the name of the protein hyphenated with the name of the corrole.

Corrole Conjugates Undergo Receptor-Targeted Cell Binding and Cell Entry

To test the binding and uptake of HerPBK10-S2Ga complexes on MDA-MB-453 cells, the complexes were incubated with the cells at 4°C to promote receptor binding but not internalization. The cells were then incubated up to 45 min at 37°C to promote endocytosis of receptors and their bound ligands. The cells were given a mild acid wash at 0 and 45 min of warming at 37°C to remove any protein remaining on the cell surface, then observed by microscopy. Cells that were kept at 4°C and not given a mild acid wash displayed fluorescence around the cell peripheries but not internally, suggesting that HerPBK10-S2Ga was bound on the cell surfaces only and not internalized (Fig. 6A and B). Endocytic inhibition at 4°C is characteristic of receptor-mediated endocytosis into clathrin-coated pits and vesicles (21). At 37°C, fluorescence can be observed within cells, indicating that the complexes have internalized (Fig. 6C and D). Importantly, this fluorescence is observed after mild acid washing, indicating that complexes have entered the cells and are protected from the acid treatment.

To test whether cell entry of HerPBK10-S2Ga is receptor-specific, we used the recombinant protein, Her, as a competitive inhibitor for heregulin receptor binding (11). HerPBK10-S2Ga complexes were coincubated with a 50× molar excess of Her (compared to HerPBK10) on MDA-MB-453 cells on ice for 30 min, then washed with buffer to remove proteins not bound to receptors. After a 5-min incubation at 37°C to induce receptor-mediated endocytosis, cells were treated with a mild acid wash to remove remaining cell surface complexes, and observed by microscopy. Cells were scored for percentage of fluorescent cells out of the total number of cells. To determine the percentage of cells taking up conjugates due to membrane damage or necrosis, cells were treated with trypan blue and scored accordingly. Whereas 10–20% of all cells took up trypan blue, nearly 80% of BSA-S2Ga-positive cells were damaged or necrotic, suggesting that cell damage accounts for a large proportion of BSA-S2Ga uptake. In contrast, nearly 20% of HerPBK10-S2Ga-positive cells were damaged, suggesting that cell damage accounts for a minority of HerPBK10-S2Ga uptake. Uptake of S2Ga in the remaining intact cells was enhanced by HerPBK10 nearly 10 times over BSA. Our findings show that a 50× molar excess of Her to HerPBK10 results in a 72% decrease in fluorescence uptake of HerPBK10-S2Ga (Fig. 6E). The same concentration of Her has no effect on BSA-S2Ga cell entry (Fig. 6E).

Altogether, these findings suggest that HerPBK10-S2Ga uptake is inhibited by low temperature, supporting a temperature-dependent receptor-mediated endocytic mechanism. Furthermore, cell binding is specific through heregulin receptors, as an excess of free Her specifically inhibits HerPBK10-mediated, but not BSA-mediated, uptake.

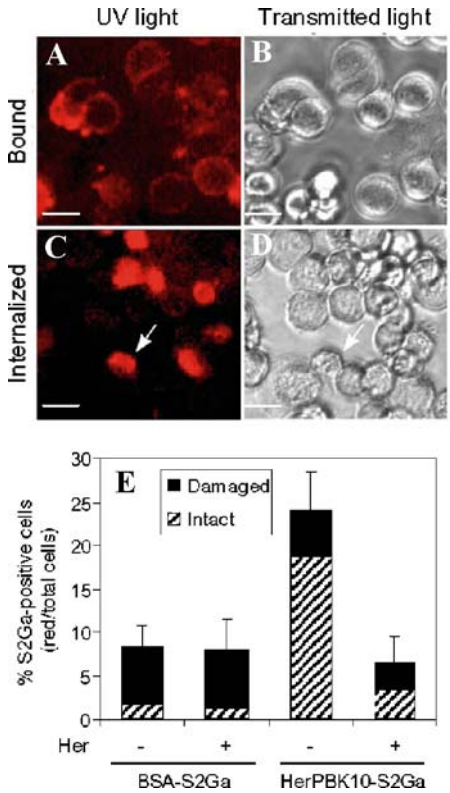

Fig. 6. HerPBK10 targets S2Ga (red fluorescence) to breast cancer cells. MDA-MB-453 cells were either: (A, B) kept at 4°C after cell binding of HerPBK10-S2Ga ("Bound"), or (C, D) warmed to 37°C after cell binding of HerPBK10-S2Ga ("Internalized"). Arrow points to a representative cell bearing internal red fluorescence after removal of cell surface molecules by acid wash. Micrographs were obtained from live cells at 10× magnification using an inverted fluorescence microscope. Bar, ~8 μm. (E) Receptor specificity of HerPBK10-S2Ga. Conjugate uptake was determined by scoring cells for red fluorescence, and damaged cells were assessed by uptake of trypan blue, as described in Materials and Methods.

Corrole Conjugates Induce Targeted Toxicity

We next examined whether HerPBK10 could induce target-specific corrole toxicity to ErbB2-positive breast cancer cells in two ways: (1) by testing targeted conjugates on ErbB2-positive and ErbB2-negative breast cancer cells; (2) by competitive inhibition of targeted toxicity using an excess molar concentration of the free ligand, Her.

HerPBK10-S2Ga or HerPBK10-S2Mn conjugates were added to ErbB2+ MDA-MB-435 or ErbB2− MDA-MB-231 cells daily at concentrations equating 0.5 μM of corrole, and cells were monitored daily for metabolic activity. Where indicated, sets of wells received the Her competitive inhibitor, which was incubated on the cells at a 10-fold molar excess (in comparison to HerPBK10 in the conjugates) before conjugate treatment.

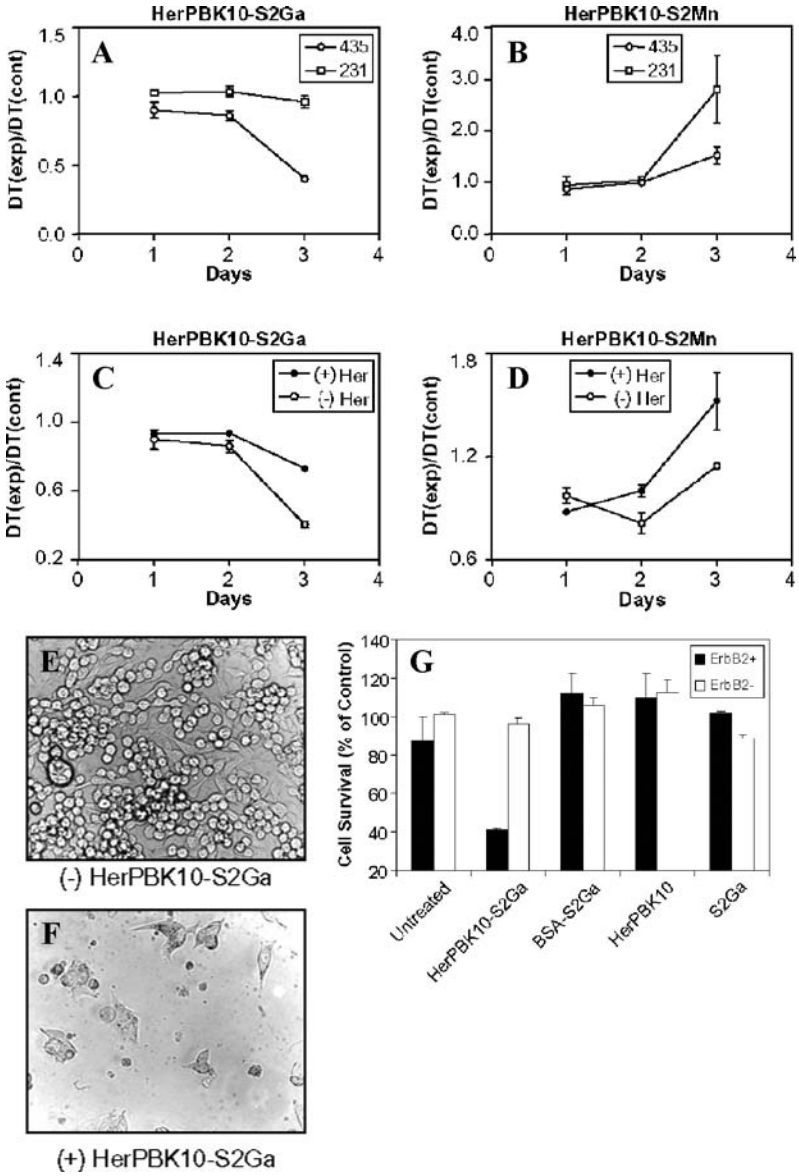

Fig. 7. Corrole conjugates induce targeted toxicity. (A–D) Toxicity is reflected by the doubling time (DT) of experimental (treated) cells normalized by that of control (untreated) cells, or DTexp/DTcont. Toxicity to ErbB2+ (MDA-MB-435) and ErbB2− (MDA-MB-231) cells induced by (A) HerPBK10-S2Ga or (B) HerPBK10-S2Mn, respectively, was measured. Free Her ligand was used to competitively inhibit targeted toxicity induced by (C) HerPBK10-S2Ga or (D) HerPBK10-S2Mn, respectively. Photomicrographs of (E) untreated or (F) treated MDA-MB-435 cells show that conjugate treatment results in a lower cell number and cytopathicity (shrinkage and lysis). (G) The HerPBK10-S2Ga conjugate induces specific cytotoxicity to ErbB2+ but not ErbB2− cells, whereas equivalent concentrations of HerPBK10 alone (0.8 μM), S2Ga alone (0.5 μM), or BSA-S2Ga alone (0.5 μM) do not. Cell survival is presented as a percentage of untreated cells.

By day 3 of the experiment, HerPBK10-S2Ga reduced the cell survival of MDA-MB-435 cells by 60% whereas survival of MDA-MB-231 cells remained unaffected (Fig. 7A and G). Likewise, HerPBK10-S2Mn slowed the growth of MDA-MB-435 cells by ~70% compared to MDA-MB-231 (Fig. 7B). As a confirmation of the targeted toxicity of the conjugates, we demonstrate here that the free ligand, Her, inhibited MDA-MB-435 cell death from HerPBK10-S2Ga by ~60–70% (Fig. 7C), and from HerPBK10-S2Mn by ~80–85% (Fig. 7D). Importantly, the conjugates seemed to induce death and lysis of the cells (Fig. 7F) as opposed to inducing cytostasis. Also importantly, neither HerPBK10 alone nor S2Ga alone produced cell death when each was applied at the equivalent molar concentrations as its cognate in the conjugate (Fig. 7G).

The toxicity induced when 0.5 μM of corrole is delivered by a targeted vehicle starkly contrasts with the toxicity induced by corroles when they are not targeted, such as when delivered alone in complete cell media, or as a BSA-S2Ga conjugate (Fig. 7G). Moreover, our previous assays indicate that cell death from nontargeted corroles did not ensue until day 6 of treatment. Taken altogether, our findings show that S2Ga can induce nearly 60% MDA-MB-435 cell death by 3 days at 0.5 μM when it is targeted, whereas the untargeted compound must be exposed to the cells for nearly a week at nearly an order of magnitude higher concentration to accomplish the same effect.

DISCUSSION

Existing approaches to targeting therapeutic compounds normally require covalent attachment of the drug to the carrier. Such an approach of chemical modification may not only complicate the preparation of the conjugate, but also compromise the potency of the drug and abrogate the activity or specificity of the carrier molecule. Instead, a system in which the therapeutic can be incorporated with a carrier and then released into the target cell would be ideal. In this study, we have explored the use of a new type of bioconjugate whereby corroles are noncovalently assembled with recombinant viral proteins having unique cell binding and entry features.

Until now, there has been little research on the effect of corroles in biological systems. Here we present the first studies on targeting noncovalent corrole assemblies to specific cell-surface receptors. In particular, the carrier molecules tested here include recombinant derivatives of the Ad5 penton base, and exhibit the functions of receptor-specific binding, cell entry, and translocation to the cytosol. Using a heregulin-directed penton base protein, we demonstrate that receptor-specific targeting of corroles to ErbB2-positive breast cancer cells, and target-specific cell death is possible.

The most significant finding in these studies is that targeted corroles induce cell death at submicromolar concentrations, whereas equivalent concentrations of the untargeted compound do not. Importantly, the protein targeting vehicle alone did not induce cell death. These findings support the premise that sulfonated corroles induce cytotoxicity only when they are able to translocate into the cell via a cell-penetrating carrier, and underscore the importance of using a targeted cell entry vehicle for effective delivery. Taken together, these findings suggest that targeting corroles using specialized carrier proteins such as HerPBK10 should enable effective dosing at reasonable concentrations while avoiding nonspecific toxicity, should the corrole release prematurely from the carrier. Given the high degree of binding stability to endure ultrafiltration, HPLC, and nonexchange with serum protein, however, this is unlikely to happen.

Among the proteins we have tested here as carriers are recombinant derivatives of the Ad5 penton base protein: PB, PBK10, and HerPBK10. The proteins PB and PBK10 enter cells by integrin receptor binding and endocytosis, and translocate into the cytoplasm by lysis of cellular endosomes (9,10). The protein, HerPBK10, utilizes the endosomolytic activity of the penton base but specifically binds and enters ErbB2-positive cells (11), which display amplified levels of the heregulin receptor on the cell surface (22,23). Taking advantage of the intense fluorescence of the S2Ga compound, we could detect both receptor-specific binding and cell entry of HerPBK10-S2Ga conjugates on ErbB2-positive human breast cancer cells.

Our findings indicate that multiple corroles noncovalently bind the recombinant proteins studied here, likely at multiple sites on the same protein molecule. The corrole binding sites on HerPBK10 or any of the other carrier molecules tested here remain to be determined. It is possible that the polyhistidine tag appended to the recombinant proteins PB, PBK10, HerPBK10, and Her, which facilitates protein purification by metal chelate chromatography, may contribute to binding. It is also possible that the positively charged polylysine on PBK10 and HerPBK10 may enable charge interactions with the sulfonates on the corroles, much the same way as these polylysines interact with the phosphate backbone of DNA (9,11). Determining which residues contribute to binding, however, is beyond the scope of this present study.

To demonstrate that HerPBK10-corrole conjugates were specifically targeted to ErbB receptors, we competitively inhibited receptor binding using excessive concentrations of free Her ligand. These concentrations equated 8–18 μM of free Her, which would be in far excess of the presumed circulating levels of heregulin (24–26). Moreover, the molarity of HerPBK10 itself when delivered as a conjugate still exceeds these levels, and thus does not present a scenario that would suggest that circulating heregulin could competitively inhibit conjugate delivery. Although Her reduced the cytotoxocity of targeted conjugates, our data suggest that S2Mn may stimulate cell doubling, which would not be a desirable effect. This apparent stimulation warrants further investigation outside the scope of this study. Considering that it may take several days to begin observing substantial reductions in cell number (Figs. 3 and 7), one possible explanation is that the cells undergo a delay in cytotoxicity, and thus may have an opportunity to divide before undergoing cell death. This finding brings up another important consideration, which is understanding the mechanism of cell death. Although corroles are capable of binding metal ions, it is unknown whether metal chelation is the actual mechanism of cytotoxicity. The actual intracellular targets of toxicity also remain to be identified. It is possible that corroles may interact with key enzymes, or may simply tightly bind intracellular protein and

thus impede function. Our future studies aim at elucidating the cell death mechanism. Meanwhile, the present studies in part explore the potential of corroles as cytotoxic drugs, and thus these findings can help us select which corroles are better candidates as anticancer compounds.

Currently used chemotherapy drugs such as doxorubicin or cisplatin exert their effect by entering the cell nucleus and binding to DNA, stabilizing certain protein–DNA complexes and resulting in inhibition of replication (27). As such, these drugs are nondiscriminatory: they can penetrate cell membranes, but induce the most potent damage on dividing cells. One of the potential advantages of amphiphilic, negatively charged corroles is their cell impermeability, as seen here. The negative charges on sulfonated corroles likely explains why these compounds are unable to enter cells without a carrier in protein-free conditions, as the net-negative charge on the cell surface would repel such corroles. Likewise, a positively charged corrole enters cells presumably because the positive charges facilitate binding to the cell surface (28). The negative charge of sulfonated corroles thus plays up an additional benefit for targeted therapy by reducing nonspecific binding to cell surfaces. This should allow for control of cell entry by conjugating corroles to certain carrier molecules.

Previous studies have tested the strategy of covalently coupling shuttle molecules, such as antibodies, to drugs but the chemical modifications introduced by this approach can reduce the activity of either component (29–31). Recombinant fusion of proteins, such as toxins, to shuttle peptides represents another strategy, but often the toxin requires special processing to become active (30,32,33). Our approach of assembling complexes as noncovalent conjugates may be superior to targeting strategies utilizing toxin fusions or covalently linked drugs, as assembly did not seem to abrogate targeting activity and, in fact, enhanced the toxicity of the corrole payload. These studies represent the first example, to our knowledge, of assembling and testing targeted corrole conjugates. These encouraging *in vitro* findings should provide a foundation for further development of targeted corrole conjugates for application in cancer therapy.

ACKNOWLEDGMENTS

We thank the following people for valuable discussions on this work: Nori Kasahara, Larry Kedes, and Renata Stripecke. This work was supported, in part, through a collaborative research agreement with IntraGene Sciences Inc., and by grants to L.K.M.-K. from the NIH (CA102126), the Susan G. Komen Breast Cancer Foundation (BCTR02-01194), and the Donna and Jesse Garber Award; to Z.G. from the STAR (Chicago) foundation; to H.B.G. from the National Science Foundation; and to I.J.D. from the Helen Hay Whitney Foundation.

REFERENCES

1. T. J. Dougherty, C. J. Gomer, B. W. Henderson, G. Jori, D. Kessel, M. Korbelik, J. Moan, and Q. Peng. Photodynamic therapy. *J. Natl. Cancer Inst.* **90**:889–905 (1998).
2. L. D. Via and S. M. Magno. Photochemotherapy in the treatment of cancer. *Curr. Med. Chem.* **8**:1405–1418 (2001).
3. T. J. Dougherty. A brief history of clinical photodynamic therapy development at Roswell Park Cancer Institute. *J. Clin. Laser Med.* **14**:219–221 (1996).
4. A. Mahammed, I. Goldberg, and Z. Gross. Highly selective chlorosulfonation of tris(pentafluorophenyl)corrole as a synthetic tool for the preparation of amphiphilic corroles and metal complexes of chiral planarity. *Org. Lett.* **3**:3443–3446 (2001).
5. I. Saltsman, A. Mahammed, I. Goldberg, E. Tkachenko, M. Botoshansky, and Z. Gross. Selective substitution of corroles: nitration, hydroformylation, and chlorosulfonation. *J. Am. Chem. Soc.* **124**:7411–7420 (2002).
6. T. G. Gantchev, R. Ouellet, and J. E. Liervan. Binding interactions and conformational changes induced by sulfonated aluminum phthalocyanines in human serum albumin. *Arch. Biochem. Biophys.* **366**:21–30 (1999).
7. R. K. Pandey, S. Constantine, T. Tsuchida, G. Zheng, C. J. Medforth, M. Aoudia, A. N. Kozyrev, M. A. Rodgers, H. Kato, K. M. Smith, and T. J. Dougherty. Synthesis, photophysical properties, *in vivo* photosensitizing efficacy, and human serum albumin binding properties of some novel bacteriochlorins. *J. Med. Chem.* **40**:2770–2779 (1997).
8. A. Mahammed, H. B. Gray, J. J. Weaver, K. Sorasaenee, and Z. Gross. Amphiphilic corroles bind tightly to human serum albumin. *Bioconjug. Chem.* **15**:738–746 (2004).
9. L. K. Medina-Kauwe, N. Kasahara, and L. Kedes. 3PO, a novel non-viral gene delivery system using engineered Ad5 penton proteins. *Gene Ther.* **8**:795–803 (2001).
10. L. K. Medina-Kauwe. Endocytosis of adenovirus and adenovirus capsid proteins. *Adv. Drug Deliv. Rev.* **55**:1485–1496 (2003).
11. L. K. Medina-Kauwe, M. Maguire, N. Kasahara, and L. Kedes. Non-viral gene delivery to human breast cancer cells by targeted Ad5 penton proteins. *Gene Ther.* **8**:1753–1761 (2001).
12. L. K. Medina-Kauwe and X. Chen. Using GFP–ligand fusions to measure receptor-mediated endocytosis in living cells. In G. Litwack (ed.), *Vitamins and Hormones, Vol. 65*, Elsevier, San Diego, 2002, pp. 81–95.
13. L. K. Medina-Kauwe, V. Leung, L. Wu, and L. Kedes. Assessing the binding and endocytosis activity of cellular receptors using GFP–ligand fusions. *BioTechniques* **29**:602–609 (2000).
14. G. S. Manning. The molecular theory of polyelectrolyte solutions with applications to the electrostatic properties of polynucleotides. *Q. Rev. Biophys.* **11**:179–246 (1978).
15. M. X. Tang and F. C. Szoka Jr. Characterization of polycation complexes with DNA. In A. V. Kabanov, P. L. Felgner, L. W. Seymour (eds.), *Self-Assembling Complexes for Gene Delivery*, Wiley, Chichester, 1998.
16. J. Zabner, A. J. Fasbender, T. Moninger, K. A. Poellinger, and M. J. Welsh. Cellular and molecular barriers to gene transfer by a cationic lipid. *J. Biol. Chem.* **270**:18997–19007 (1995).
17. G. L. Lukacs, P. Haggie, O. Seksek, D. Lechardeur, N. Freedman, and A. S. Verkman. Size-dependent DNA mobility in cytoplasm and nucleus. *J. Biol. Chem.* **275**:1625–1629 (2000).
18. L. Karayan, B. Gay, J. Gerfaux, and P. A. Boulanger. Oligomerization of recombinant penton base of adenovirus type 2 and its assembly with fiber in baculovirus-infected cells. *Virology* **202**:782–795 (1994).
19. T. J. Wickham, P. Mathias, D. A. Cheresh, and G. R. Nemerow. Integrins avb3 and avb5 promote adenovirus internalization but not virus attachment. *Cell* **73**:309–319 (1993).
20. A. Mahammed and Z. Gross. Aluminum corrolin, a novel chlorophyll analogue. *J. Inorg. Biochem.* **88**:305–309 (2002).
21. S. Mukherjee, R. N. Ghosh, and F. R. Maxfield. Endocytosis. *Physiol. Rev.* **77**:759–803 (1997).
22. D. J. Slamon, G. M. Clark, S. G. Wong, W. J. Levin, A. Ullrich, and W. L. McGuire. Human breast cancer: correlation of relapse and survival with amplification of the HER-2/neu oncogene. *Science* **235**:177–182 (1987).
23. D. J. Slamon and G. M. Clark. Amplification of c-erbB-2 and aggressive human breast tumors? *Science* **240**:1795–1798 (1988).
24. W. E. Holmes, M. X. Sliwkowski, R. W. Akita, W. J. Henzel, J. Lee, J. W. Park, D. Yansura, N. Abadi, H. Raab, and G. D. Lewis *et al.* Identification of heregulin, a specific activator of p185erbB2. *Science* **256**:1205–1210 (1992).
25. S. D. Chan, D. M. Antoniucci, K. S. Fok, M. L. Alajoki, R. N. Harkins, S. A. Thompson, and H. G. Wada. Heregulin activation

of extracellular acidification in mammary carcinoma cells is associated with expression of HER2 and HER3. *J. Biol. Chem.* **270**:22608–22613 (1995).
26. V. R. Schelfhout, E. D. Coene, B. Delaey, A. A. Waeytens, L. De Rycke, M. Deleu, and C. R. De Potter. The role of heregulin-alpha as a motility factor and amphiregulin as a growth factor in wound healing. *J. Pathol.* **198**:523–533 (2002).
27. L. H. Hurley. DNA and its associated processes as targets for cancer therapy. *Nat. Rev.* **2**:188–200 (2002).
28. D. Aviezer, S. Cotton, M. David, A. Segev, N. Khaselev, N. Galili, Z. Gross, and A. Yayon. Porphyrin analogues as novel antagonists of fibroblast growth factor and vascular endothelial growth factor receptor binding that inhibit endothelial cell proliferation, tumor progression, and metastasis. *Cancer Res.* **60**:2973–2980 (2000).
29. K. A. Chester, J. Bhatia, G. Boxer, S. P. Cooke, A. A. Flynn, A. Huhalov, A. Mayer, R. B. Pedley, L. Robson, S. K. Sharma, D. I. Spencer, and R. H. Begent. Clinical applications of phage-derived sFvs and sFv fusion proteins. *Dis. Markers* **16**:53–62 (2000).
30. A. E. Frankel, R. J. Kreitman, and E. A. Sausville. Targeted toxins. *Clin. Cancer Res.* **6**:326–334 (2000).
31. M. E. Reff and C. Heard. A review of modifications to recombinant antibodies: attempt to increase efficacy in oncology applications. *Crit. Rev. Oncol. Hematol.* **40**:25–35 (2001).
32. M. Schmidt, M. Maurer-Gebhard, B. Groner, G. Kohler, G. Brochmann-Santos, and W. Wels. Suppression of metastasis formation by a recombinant single chain antibody-toxin targeted to full-length and oncogenic variant EGF receptors. *Oncogene* **18**:1711–1721 (1999).
33. M. Jeschke, W. Wels, W. Dengler, R. Imber, E. Stocklin, and B. Groner. Targeted inhibition of tumor-cell growth by recombinant heregulin–toxin fusion proteins. *Int. J. Cancer* **60**:730–739 (1995).